Chapter 6
Manipulation of Neural Circuits in *Drosophila* Larvae

Ibrahim Tastekin and Matthieu Louis

Abstract *Drosophila* has proven to be an extraordinarily prolific model organism to study the integrated function of neural circuits. This success largely stems from the development of powerful genetic tools to monitor and to manipulate the activity of identified neurons in the fly nervous system. However, establishing causal relationships between the activity of a given neuron and the expression of a behavior remains challenging both at a technical and at a conceptual level. First, the characterization of behavioral phenotypes still lacks standardization in the field. Here, we illustrate the importance of quantitative analysis of behaviors as complex as sensory navigation (chemotaxis). Second, experimenters are often confronted with the absence of suitable reagents to exclusively label their neurons of interest. A driver line associated with an interesting loss- or gain-of-function phenotype often covers a heterogeneous group of neurons. In the present chapter, we describe how reagents freely available to the fly community can be combined to nail down the relationships between phenotypic traits and the activity of single neurons.

6.1 Introduction

The *Drosophila* larva is a premier model organism to delineate computational principles underlying how neural circuits transform sensory inputs into stereotyped behaviors. Traditionally, neuroscientists study circuit computation by breaking

I. Tastekin · M. Louis (✉)
EMBL/CRG Systems Biology Research Unit, Centre for Genomic Regulation (CRG),
The Barcelona Institute of Science and Technology, Dr. Aiguader 88,
08003 Barcelona, Spain
e-mail: mlouis@lifesci.ucsb.edu

I. Tastekin · M. Louis
Universitat Pompeu Fabra (UPF), 08002 Barcelona, Spain

M. Louis
Neuroscience Research Institute and Department of Molecular, Cellular and Developmental Biology, University of California Santa Barbara, 93106 Santa Barbara, California, USA

A. Çelik and M.F. Wernet (eds.), *Decoding Neural Circuit Structure and Function*, DOI 10.1007/978-3-319-57363-2_6

neural circuits down into their core components—individual neurons (invertebrates) or neuronal cell types (vertebrates)—and by testing the necessity and sufficiency of individual neurons to execute a behavior. The combination of community-based reconstruction of the whole larval brain connectivity based on light and electron microscopy (Li et al. 2014; Schneider-Mizell et al. 2016) and the presence of sophisticated genetic tools makes the larva particularly suited to progress from "circuit mapping" to a holistic "circuit cracking" (Olsen and Wilson 2008). The larva combines other advantages for circuit cracking: it has a small heat capacity facilitating thermogenetic manipulations. It is mostly transparent, which is convenient for optogenetic gain-of-function experiments and live imaging. The larva displays stereotyped behaviors on a timescale considerably slower than adult flies (Green et al. 1983). In addition, foraging in the larva can be studied on two-dimensional substrates as basic as an agarose slab instead of complex tri-dimensional environments. As a result, tracking naturalistic behaviors is technically simpler in the larva than in the adult fly.

While the numerical complexity of the nervous system of the larva is reduced by one order of a magnitude compared to its the adult fly counterpart (10,000 vs. 100,000 neurons), the *Drosophila* larva exhibits sensory-driven reorientation maneuvers in chemical, light, and temperature gradients as well as robust escape behaviors in response to threatening stimuli (Hwang et al. 2007; Luo et al. 2010; Kane et al. 2013; Zhang et al. 2013; Ebrahim et al. 2015). The larva is also capable of forming and retrieving associative memory (Gerber and Stocker 2007). The control of reorientation behavior is plastic: it can be modulated by memory traces (Schleyer et al. 2015). Genetic tools provide access to visualize and manipulate the function of small groups or even individual neurons. These tools can be efficiently combined with electron microscopy (EM) reconstruction of the entire larval brain to build circuit-level connectivity diagrams (Ohyama et al. 2015; Schneider-Mizell et al. 2016; Zwart et al. 2016). One can perform "circuit epistasis" by hierarchically manipulating different cell types revealed by EM connectivity diagrams (Ohyama et al. 2015). Altogether, recent advances in the field of larval neurobiology have created unprecedented opportunities to unravel the operation of neural circuits and to test mechanistic hypotheses with a spatiotemporal resolution that will soon match the same standards as in *C. elegans*.

The main objective of this book chapter is to review current genetic tools to manipulate neural functions in the *Drosophila* larva. First, we will draw the attention of the reader on the promises and the limitations of existing tools to study the function of individual neurons. Second, we will discuss the importance of quantifying behavior to search for the neural correlates of sensorimotor functions (Egnor and Branson 2016). Third, we will describe clonal gain-of-function strategies to dissect the contribution of distinct groups of neurons labeled by a driver line associated with a phenotype of interest. This method is intended to make the most out of driver lines with expression patterns that cover more than a couple of neurons—a problem "*Drosophilists*" frequently face when they analyze the neural mechanisms underlying the organization of behavior.

6.2 Genetic Targeting of Neurons in the *Drosophila* Larva

In *Drosophila,* high stereotypy of morphology and connectivity of individual cell types allow the analysis of neural function at a population level. Transgenic expression of reporters and/or effectors in subsets of neurons via binary expression systems has been widely used to visualize and to functionally manipulate specific neurons (Venken et al. 2011). Recently, two large collections of Gal4 driver lines (Pfeiffer et al. 2008; Bidaye et al. 2014) have been created and made accessible to the fly community to label reproducible subsets of neurons in the *Drosophila* brain. Despite the fact that these driver lines label relatively small numbers of neurons compared to their predecessors (e.g., the so-called Kyoto collection), anatomical and behavioral experiments often necessitate targeting even smaller subsets of neurons—ideally single neurons. Stochastic labeling methods such as flip-out, MARCM (Venken et al. 2011) and multicolor flip-out (MCFO) (Nern et al. 2015) have been used to characterize the morphology of single neurons using Gal4 driver lines. For behavioral studies, intersectional expression combining Gal4, Gal80, LexA expression systems, and the Split-Gal4 technique (Luan et al. 2006; Pfeiffer et al. 2010) are now routinely used to restrict expression to predefined subsets of neurons (Aso et al. 2014; Hampel et al. 2015; Ohyama et al. 2015). However, these intersectional techniques are limited by the existence of driver lines with overlapping expression patterns. In the following sections, we will describe how driver lines with expression patterns including more than one neuron can be exploited to draw hypotheses about the link between connectivity and function in specific neurons.

6.3 Inferring Function by Manipulating the Activity of Genetically Labeled Neurons

Traditionally, behavioral experiments are conducted to test the necessity or sufficiency of neurons to execute a certain type of behavior in *Drosophila* (Vogelstein et al. 2014; Tastekin et al. 2015). In many cases, the necessity of a neuron to control a given function is probed by (i) hyperpolarizing the neuron upon overexpression of the inward-rectifier potassium ion channel Kir2.1 (Baines et al. 2001) or by (ii) blocking synaptic transmission with tetanus toxin light chain (TNT) (Sweeney et al. 1995) or the temperature-sensitive dynamin mutant *shibire* (Thum et al. 2006). Caution must be taken while interpreting the results that follow the expression of an effector that is supposed to inhibit neural function. One should keep in mind that TNT impairs the release of neurotransmitter by cleaving neuronal synaptobrevin, a protein necessary for calcium-dependent vesicle fusion (Sweeney et al. 1995; Baines et al. 2001). As a result, TNT does not affect synaptic transmission mediated by pathways independent of synaptobrevin (Thum et al. 2006). In addition, it has been argued that blockage of synaptic transmission affects the electrical

development of neurons (Baines et al. 2001). Accordingly, prolonged expression of TNT might lead to compensatory effects at the neuronal and/or circuit level. While UAS constructs inserted in different genomic sites can produce different expression patterns (Aso et al. 2014), expression pattern of a given driver line can vary depending on the reporter it is coupled with (Fig. 6.1). In light of this, co-expressing TNT and fluorescent indicators by using different UAS transgenes does not guarantee a perfect correlation in the resulting expression patterns. One should therefore remember that the expression of a fluorescent indicator might not faithfully reproduce that of TNT. The fact that a tagged version of TNT does not exist makes it difficult to determine whether TNT is expressed in the targeted neurons. Fortunately, a GFP-tagged version of Kir2.1 exists. Although constant hyperpolarization might lead to compensatory effects at the circuit level, it has been shown that expression of Kir2.1 does not lead to a change in the electrical properties of at least two types of motor neurons in the larva (aCC and RP2), suggesting that Kir2.1 expression does not change the electrical properties of a neuron (Baines et al. 2001).

In comparison with TNT and Kir2.1, the dominant-negative allele *shibire*^{ts} offers temporal control, which permits to overcome the compensatory and developmental effects of chronic inhibition. Using *shibire*^{ts}, synaptic release can be reversibly blocked under restrictive temperatures (29–34 °C). One has to remain careful while interpreting the effects of manipulations involving *shibire*^{ts} since the expression of this reagent can induce morphological changes (Gonzalez-Bellido et al. 2009). Another caveat with the use of temperature changes is the interference with innate temperature-driven behaviors (thermotaxis). The outcome of temperature increases is therefore composite: it results from the effects of synaptic transmission block and the innate response to thermal stimulation. Moreover, heat convection induced by temperature changes in the assay can perturb the geometry of any odor gradient it might enclose. For this reason, it is preferable to avoid using effectors requiring temperature changes while testing the necessity of specific sets of neurons to direct orientation behaviors such as chemotaxis (Fig. 6.2a). Toxins (e.g., diphtheria toxin) and proapoptotic genes (e.g., *Reaper* and *Head involution defective*) are more rarely used to block neural function by inducing cell death. Their lack of popularity is mainly due to the detrimental effects that cell death can have on the development of the rest of the brain. For a more detailed discussion of the reagents commonly used to dissect neural function, we refer the reader to two thorough reviews (Simpson 2009; Venken et al. 2011). Upon applications of effectors inducing a loss of function, the effects of impairing the function of a given neuron or a neuronal subset should be always interpreted at the circuit level. In addition, the nonlinear dynamics generated by networks of interconnected cells imply that neural circuits must produce complex behaviors that cannot be inferred from the effects of blocking parts of the circuits.

Sufficiency is usually defined by whether activation of a given neuron triggers a certain type of behavior or the response of a putative downstream partner. Acute activation of neurons in the larva has been successfully accomplished by using thermogenetic and optogenetic tools (Pulver et al. 2009). Targeted expression of

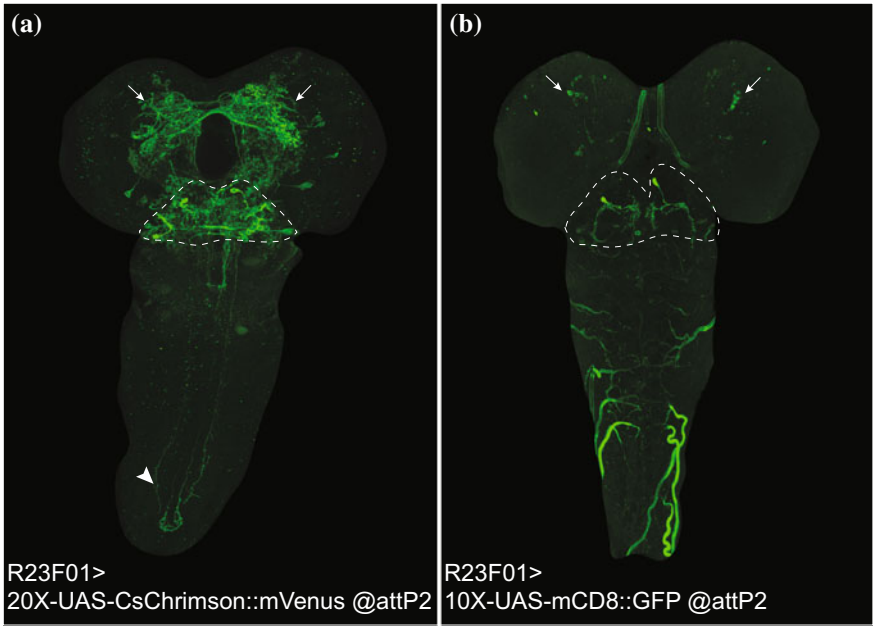

Fig. 6.1 Variability in the expression pattern of the same GAL4 driver line reported by two different UAS transgenes inserted in the same landing site. **a** Expression pattern of R23F01>20X-UAS-IVS-CsChrimson::mVenus. Both R23F01 and 20X-UAS-IVS-CsChrimson::mVenus transgenes are inserted at the attP2 landing site on the 3rd chromosome. *Dashed line* encloses the subesophageal zone (*SEZ*). Note the high level of expression of the reporter in the SEZ. *Arrows* highlight expression in the brain lobes. The large *arrowhead* indicates the axon of a descending neuron from the SEZ. **b** Expression pattern of R23F01>10X-UAS-IVS-mCD8::GFP (retrieved from http://flweb.janelia.org/cgi-bin/flew.cgi). Both R23F01 and 10X-UAS-IVS-mCD8::GFP transgenes are inserted at the attP2 landing site on the 3rd chromosome. *Dashed line* encloses the subesophageal zone (*SEZ*). In contrast with panel **a**, only two neurons are labeled in the SEZ and very few Kenyon cells are labeled in each brain lobe. The picture shown in panel **b** is courtesy of the Truman lab (Li et al. 2014). It is reproduced with the permission of the author

Drosophila TrpA1 (dTrpA1) channel (Rosenzweig et al. 2008) has been widely used to activate neurons upon temperature increases. Although this tool has proved to be useful to induce stereotypic behavioral sequences in adult flies (von Philipsborn et al. 2011; Marella et al. 2012), it lacks both temporal resolution and control over the intensity ranges of the neural activity. This is particularly important as the level and timing of a gain in neural activity might trigger distinct behavioral output due to complex circuit interactions. It has to be noticed that continuous activation of dTrpA1 might lead to a depolarization block in some neurons via rapid depolarization (Inagaki et al. 2014). Furthermore, temperature manipulations necessary to activate neurons might create behavioral interferences induced by innate responses to temperature changes, as indicated above. In recent work on the sensorimotor control of larval chemotaxis (Tastekin et al. 2015), we were unable to

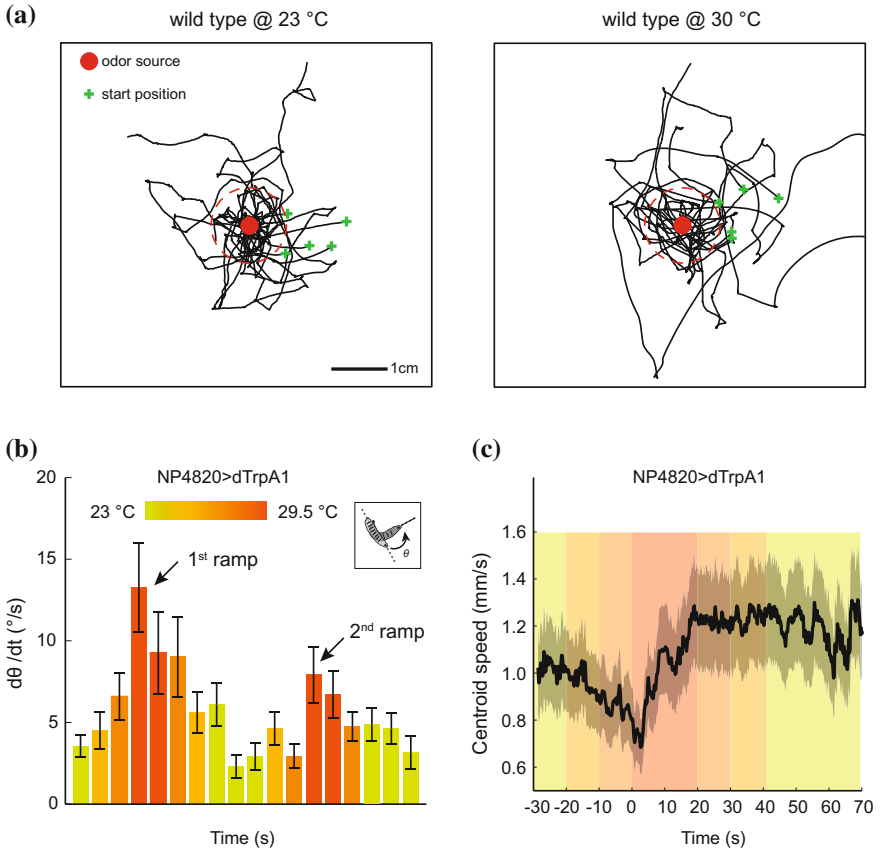

Fig. 6.2 Thermogenetic gain-of-function manipulations in the *Drosophila* larva. **a** Effect of temperature on larval chemotaxis. An odor gradient is formed by using a point odor source (*red dots*, 10 μL of a 100-μM solution of ethyl butyrate). Trajectories from 5 representative larvae were plotted for 23 °C (*left panel*) and 30 °C (*right panel*). Note that wild type larvae tend to stay closer to the odor source when they are allowed to chemotax at 23 °C. **b** Thermogenetic activation of NP4820-labeled neurons by expressing dTrpA1 reagent. Temperature is raised slowly from 23 to 29.5 °C in a period of 30 s and subsequently decreased back to 23 °C. The temperature ramp is repeated twice. Activation of NP4820-labeled neurons led to a transient increase in average head angular speed (head sweeps) during the first temperature increase phase of the temperature (*arrow*). However robust head sweeps cannot be elicited during the second increase in temperature (*arrow* labeled as 2nd ramp). Each *bar* indicates average head angular speed binned in 10-s windows. *Error bars* indicate standard errors of the mean. **c** Thermogenetic activation of NP4820-labeled neurons leads to a transient increase in head sweeps followed by fast crawling. Increase in centroid speed is observed shortly after thermogenetic activation. The *shaded boxes* of different *colors* (see *horizontal* heat map *bar* in **b** for corresponding temperature scale) represent the windows of time during which the temperature was brought from 23 to 29.5 °C

trigger a reproducible gain-of-function phenotype using thermogenetics (Fig. 6.2b) while optogenetic activation led to a strong and reliable phenotype in single larvae. In the next paragraphs, we will argue that the use of optogenetics has multiple advantages compared to thermogenetics.

Due to its superior temporal precision, optogenetic activation has become increasingly adopted for gain-of-function manipulations aiming to test sufficiency (Fenno et al. 2011). Until recently, the performances of Channelrhodopsin 2 (ChR2), a blue light gated ion channel, were limited in *Drosophila* for several reasons including the low penetrance of blue light through the cuticle of adult flies and the innate responses of the adults and the larvae. In spite of this limitation, ChR2 has been successfully applied to study proboscis extension, escape responses, learning, locomotor activity (Schroll et al. 2006; Gordon and Scott 2009; Zimmermann et al. 2009; Matsunaga et al. 2013), and orientation behaviors (Zhang et al. 2007; Gepner et al. 2015; Hernandez-Nunez et al. 2015; Schulze et al. 2015). Since the function of ChR2 necessitates its coupling with the chromophore all-trans retinal that is not endogenously produced by *Drosophila*, larvae must be grown in food complemented with all-trans retinal. Note however that a small amount of retinal is present in regular fly food (Claire McKellar, personal communication). Recent development of red-shifted optogenetic tools (ReaChr, CsChrimson and ChrimsonR) (Inagaki et al. 2014; Klapoetke et al. 2014) enabled deeper penetration of light as well as minimal innate response to visual stimulation, which opened new avenues in *Drosophila* optogenetics. It has been shown that ChrimsonR has relatively higher off kinetics compared to CsChrimson and it can produce sustained trains of spikes when activated at moderately high frequencies (20 Hz) (Klapoetke et al. 2014).

Drosophila larvae are averse to blue light during most of their development (Kane et al. 2013). Abrupt changes in blue light intensity lead to increased turning. On the other hand, we observed that wild type *Drosophila* larvae show minimal to no response to changes in light intensity at 625 nm when they are fed on food with all-trans retinal (Fig. 6.3a, b) while 0.3–3 W/m^2 is sufficient to induce paralysis when CsChrimson is expressed in most of the motor neurons using OK6-Gal4 (Fig. 6.3f). In our hands, much higher light intensities had to be applied to activate brain interneurons (10–18 W/m^2, Fig. 6.3c, d). We observed that reproducible behavioral responses could be elicited over several trials using CsChrimson. However, we noted occasional time-dependent decreases in behavioral response upon the application of prolonged light stimulations (data not shown). This dampening of the gain of function is probably due to the off kinetics of CsChrimson and its slower recovery. It might also be related to the dynamics of the host neuron(s) independently of the effector. Therefore, the kinetics of the effector—whether it is CsChrimson, ChrimsonR or ChR2—should be carefully considered when choosing the duration and frequency of optogenetic stimulations. In case stimulation at high frequencies is required, ChrimsonR should be favored over CsChrimson.

In the *Drosophila* larva, large-scale screens testing loss of functions (necessity) and gain of functions (sufficiency) have been performed to identify neural correlates

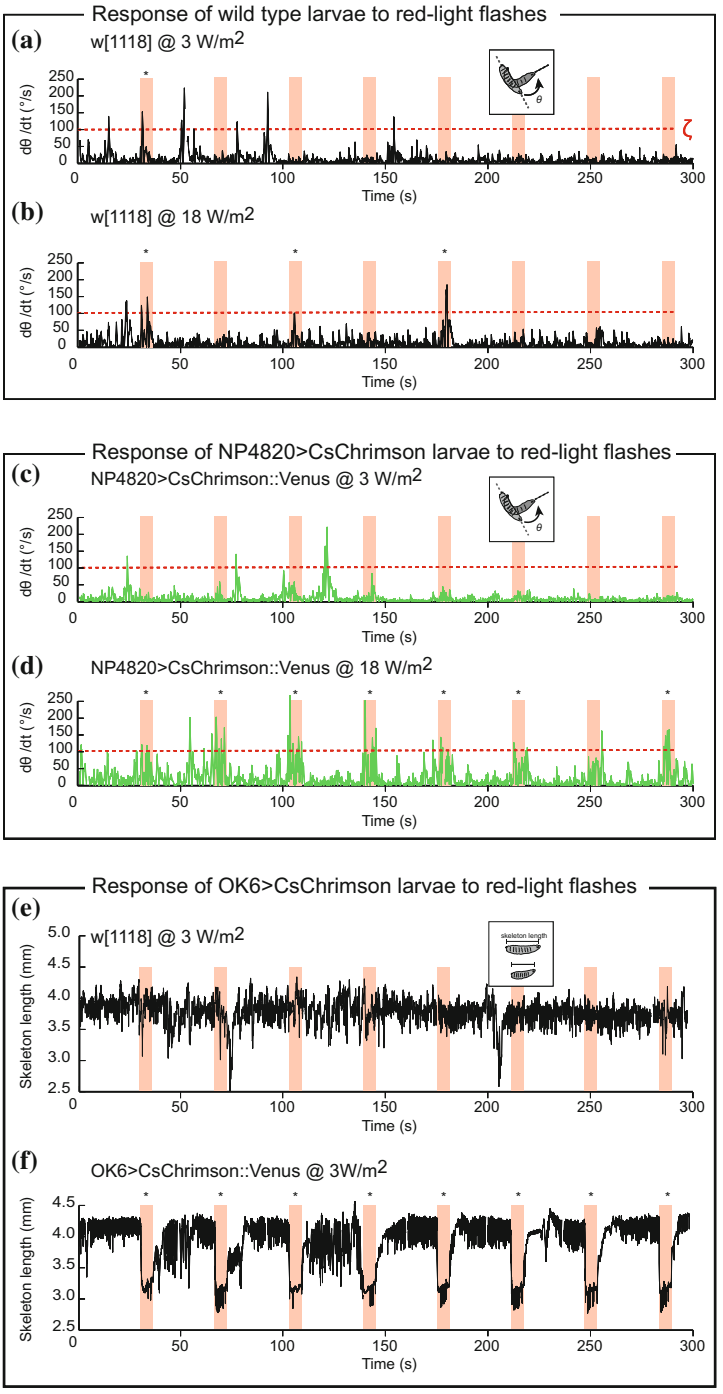
Response of wild type larvae to red-light flashes
(a)
w[1118] @ 3 W/m2
dθ /dt (°/s)
Time (s)
(b)
w[1118] @ 18 W/m2
Response of NP4820>CsChrimson larvae to red-light flashes
(c)
NP4820>CsChrimson::Venus @ 3 W/m2
(d)
NP4820>CsChrimson::Venus @ 18 W/m2
Response of OK6>CsChrimson larvae to red-light flashes
(e)
w[1118] @ 3 W/m2
Skeleton length (mm)
(f)
OK6>CsChrimson::Venus @ 3W/m2

◂**Fig. 6.3** Innate sensitivity of larvae to *red light* and acute optogenetic activation of neural activity using CsChrimson. **a** We probe the response of the control larvae subjected to 6-s flashes of *red light* (625 nm) at an intensity of 3 W/m^2. The behavioral response is defined by quantifying head sweeps as a function of the angular speed. A head sweep is considered to be a "cast" when the absolute value of the angular speed exceeded a threshold ζ of 100°/s. For more information about the method used to determine the value of threshold on the head angular speed, see Fig. 6.5. The genotype used is w[1118], which corresponds to one of the most common genetic background for transgenics. At low light intensity, w[1118] only occasionally performs head sweeps that qualify as head casts (*stars* 1 out of 8 flashes). **b** Same as panel **a** with a higher intensity (18 W/m^2) of *red light*. Head sweeps more frequently qualify as head casts than at a lower intensity of 3 W/m^2 (*stars* 3 out of 8 flashes). **c** Optogenetic activation of the NP4820-labeled neurons with 3 W/m^2 of *red light* (625 nm) upon expression of CsChrimson. Same pattern of light flashes as shown in panel **a**. The larva does not respond to *red light* at this intensity. **d** Same as **c** with 18 W/m^2 intensity. Robust head casts are observed as a function of absolute head angular speed (*stars* 6 out of 8 flashes). In panels **c** and **d**, larvae were raised on regular fly food with a concentration of 0.5 mM all-trans retinal. **e** Response of control larvae w[1118] subjected to 6-s flashes of *red light* at an intensity of 3 W/m^2. Quantification of the behavioral response by the length of larva's skeleton. *Red light* flashes of 3 W/m^2 intensity do produce a significant decrease in body length. **f** Optogenetic activation of OK6 neurons with 3 W/m^2 of *red light*. OK6 covers most of the motor neurons in the VNC. As a result of the global activation of motor neurons, muscles across the body length contract simultaneously leading to significant decrease in the skeleton length

of behavioral control (Vogelstein et al. 2014; Tastekin et al. 2015; Clark et al. 2016; Yoshikawa et al. 2016). The number of neurons typically covered by a driver line that led to a phenotype ranged from one to a few dozens. Instead of treating each labeled neuron as a separate unit, it is convenient to group neurons by lineages. Lineages from circuit elements can be viewed as the anatomical building blocks of the brain (Hartenstein et al. 2015). For some of the hits identified in screens, an interesting behavioral phenotype could not be mapped on a single lineage due to the existence of multiple lineages covered by the driver line yielding the phenotype of interest. In these cases, alternative strategies have been deployed to restrict the phenotype to the activation/silencing of a single cell type. For example, Ohyama and colleagues successfully utilized a combination of two binary expression systems (Gal4 and LexA) together with the Split Gal4 technique to narrow down the mapping of a behavioral phenotype onto one or a small set of lineages (Ohyama et al. 2015). This approach relies on the existence or the generation of combinations of Split Gal4 lines, which is not always possible.

In recent work, we adopted a different strategy to uncover circuit elements participating in the sensory control of the timing of turning maneuvers (Tastekin et al. 2015). In this study, we used a densely expressed Gal4 driver line (multiple cell types with more than 50 neurons in the brain lobes and the subesophageal zone). Our attempts to confine the expression of the driver line to a few neurons using traditional Gal80 and lexA intersections could only lead to the conclusion that one or more cells out of a group of $\sim$15 located in the subesophageal zone (SEZ) are responsible for the gain of function phenotype (triggering of a turning maneuver). To enhance the precision of the circuit-function mapping, we applied an acute gain-of-function strategy combined with random labeling of neurons. We

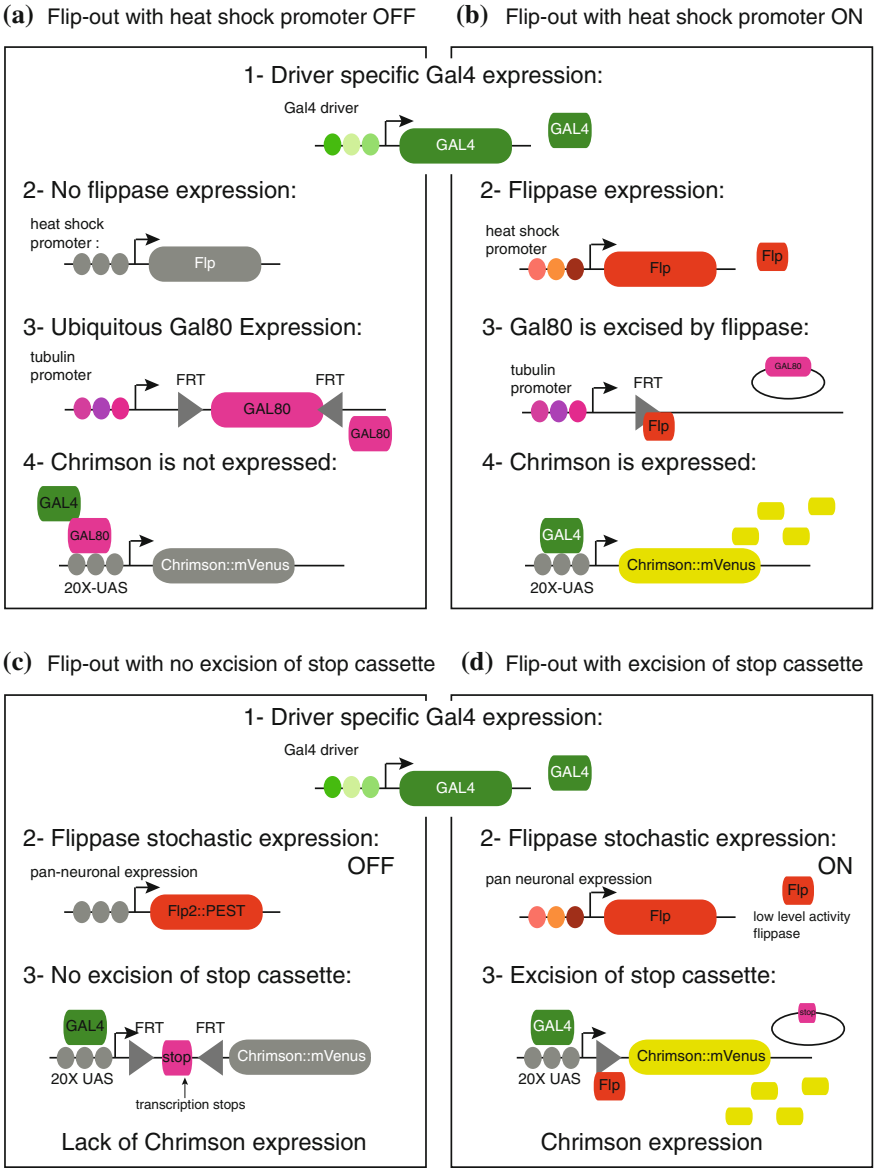

induced stochastic expression of Chrimson::mVenus in small subsets of neurons by combining the original densely expressed Gal4 driver line with a Gal80 driver whose expression was conditioned by a probabilistic flip-out recombination under the control of a heat shock promoter (Fig. 6.4a, b). After performing acute activation of each clone, we visualized the expression of Chrimson protein in individual clones using standard immunostaining against mVenus protein. In this way,

◂**Fig. 6.4** Two different flip-out intersectional strategies to stochastically express CsChrimson::mVenus in clones. **a**, **b** "Flip-out" strategy mediated by heat shock (*hs*) promoter. In panel **a**, the hs promoter is OFF. As a consequence, Gal80 flanked by FRT is ubiquitously expressed under the control of tubulin promoter and inhibits Gal4-UAS dependent expression of CsChrimson::mVenus. In panel **b**, the hs promoter is ON, which drives expression of the flippase protein. Flippase excises the Gal80 sequence, thereby abolishing ubiquitous Gal80 expression. Gal4 can bind to the UAS sequences and drive CsChrimson::mVenus expression in a cell-specific manner. **c**, **d** "Flip-out" strategy using pan-neuronal expression of low-level activity version of flippase (Flp2::PEST, for details see Nern et al. 2015). A transcriptional stop cassette flanked with FRT was placed between UAS and CsChrimson::mVenus sequences preventing Gal4-dependent expression of CsChrimson::mVenus in the absence of sufficient flippase activity (panel **c**). In panel **d**, the higher level of activity of flippase in some cells is sufficient to excise the stop cassette upstream from the coding sequence of CsChrimson::mVenus. As a result, CsChrimson::mVenus is expressed in a subset of cells of the original pattern labeled by the Gal4 driver

we could directly monitor the expression of the effector (CsChrimson). This approach is more reliable than indirectly assessing the expression of an effector (e.g., TNT) through an additional reporter (e.g., UAS-GFP). As described in the next section, we devised a statistical method to correlate gain-of-function behaviors with expression patterns of CsChrimson. Below, we will detail this approach as it represents a useful alternative to infer circuit function relationships associated with Gal4 lines expressed in multiple lineages when sparse driver lines do not exist to reduce the expression pattern of the original driver line.

6.4 Stochastic Labeling of Neurons Using Flip-Out Approach

The flip-out method has been widely used to stochastically visualize subsets of neurons covered by Gal4 drivers (Venken et al. 2011). We employed a similar strategy based on the "FLP-FRT" recombination system (Fig. 6.4). Following a first variant of this approach, the expression of Gal80 flanked by FRT sequences is induced ubiquitously by a tubulin promoter (FLP-out Gal80) (Gordon and Scott 2009). When the flippase (FLP) recombinase is stochastically expressed under the control of a heat shock promoter, it stochastically induces excision of the FRT-Gal80-FRT cassette downstream of the tubulin promoter. As a result, Gal80 is not expressed in the subset of neurons where the recombination took place, thereby allowing full activity of Gal4 and expression of the effector (e.g., Chrimson::mVenus). This method was initially applied to stochastically silence/activate neurons involved in proboscis extension in adult flies (Gordon and Scott 2009). It enables lineage-independent expression of effectors in different combinations of neurons and it is possible to optimize the probability of flip-out events by changing the strength and duration of the heat shock. Thus, one can roughly control the number of cells in which the effector expression is allowed by the heat shock induced loss of Gal80.

Fig. 6.5 Stochastic labeling of subsets of neurons in gain-of-function clones of the NP4820-Gal4 ► driver line. **a**, **b** Two clones showing expression in subsets of neurons upon heat-shock-dependent stochastic expression (see method described in Fig. 6.4a, b). *Arrows* indicate neurons that are functional in larvae at the third developmental stage. Stars indicate immature secondary lineage neurons that are unlikely to be functional at the third instar stage. Panel **a** features a clone without a behavioral phenotype while the brain displayed in panel **b** demonstrated a strong gain-of-function phenotype (see text for the explanation of positive and negative phenotypes). **a'**, **b'** Quantification of the behavioral phenotype observed upon acute optogenetic gain of function of the clones shown in panels **a** and **b**, respectively. The trace of panel **a'** is associated with a negative phenotype since the larva does not respond to any of the light flashes. Panel **b'** is associated with a positive phenotype since the larva demonstrated a strong increase in head angular speed ($d\theta/dt$) that exceeded the threshold ζ for 7 out of the 8 flashes. **c** Receiver operating characteristic *curve* used to define a binary classifier for efficient detection of behaviorally positive clones. "Responsivity" is defined as the number of flashes during which head angular speed exceeds a certain threshold value (ζ). Responsivity ranges between 1 and 8. In panel **c**, the ROC analysis corresponds to a responsivity of 6. The ROC is plotted for different ζ values ranging from 10 to 180°/s (*gray circles*). Optimal classification (true positive TP rate is as high as possible and false positive FP rate is as low as possible) was obtained at responsivity = 6 and for a ζ value of 100°/s (*red circle*). Using these criteria, the number of false positives expected for a batch of 70 tested larvae is $0.04 \times 70 = 3$ individuals. **d** Comparison of the ROC corresponding to a responsivity of 5 flashes (*red curve*) and 6 flashes (*blue curve*). For both responsivity, the ROC is shown for values of ζ ranging from 10 to 180°/s

One disadvantage of this flip-out approach is that hs-flp transgene and the tubulin promoter-FRT-Gal80-FRT transgene cannot be combined in the same fly stock since excision of Gal80 might occur in the germ line and lead to an irreversible loss of Gal80 in the offspring. For this reason, a new transgene must be generated for each Gal4 driver line. In order to activate and visualize the neurons that are stochastically labeled, we used red-shifted opsin CsChrimson (Klapoetke et al. 2014) fused to fluorescent protein mVenus (a collection of CsChrimson::mVenus effector inserted in different landing sites have been generated by Vivek Jayaraman; these reagents are available from the Bloomington stock center). For thermogenetic activation and subsequent visualization of the effector, dTrpA1::myc-tag fusion can be used (dTRPA1^{myc}) (von Philipsborn et al. 2011).

An alternative flip-out strategy relies on the expression of a weakened version of FLP recombinase under the control of a pan-neuronal driver (Nern et al. 2015). In this method, expression of the FLP recombinase is restricted to the differentiated neurons by driving the expression of FLP with the promoter of N-synaptobrevin gene (R57C10) (Jenett et al. 2012). Instead of flanking ubiquitously expressed Gal80, a transcriptional stop cassette flanked by FRT (Wong et al. 2002) was introduced between UAS and CsChrimson::mVenus (dTRPA1^{myc} or dTRPA1^{mcherry} in case of thermogenetics) (von Philipsborn et al. 2011; Asahina et al. 2014). Low-level pan-neuronal expression of weakened FLP recombinase is expected to yield stochastic expression of CsChrimson::mVenus protein in a small subset of neurons (Fig. 6.4c, d). Unlike the Gal80-based method, R57C10-FLP and UAS-FRT-stop-FRT-CsChrimson::mVenus transgenes can be combined in a single

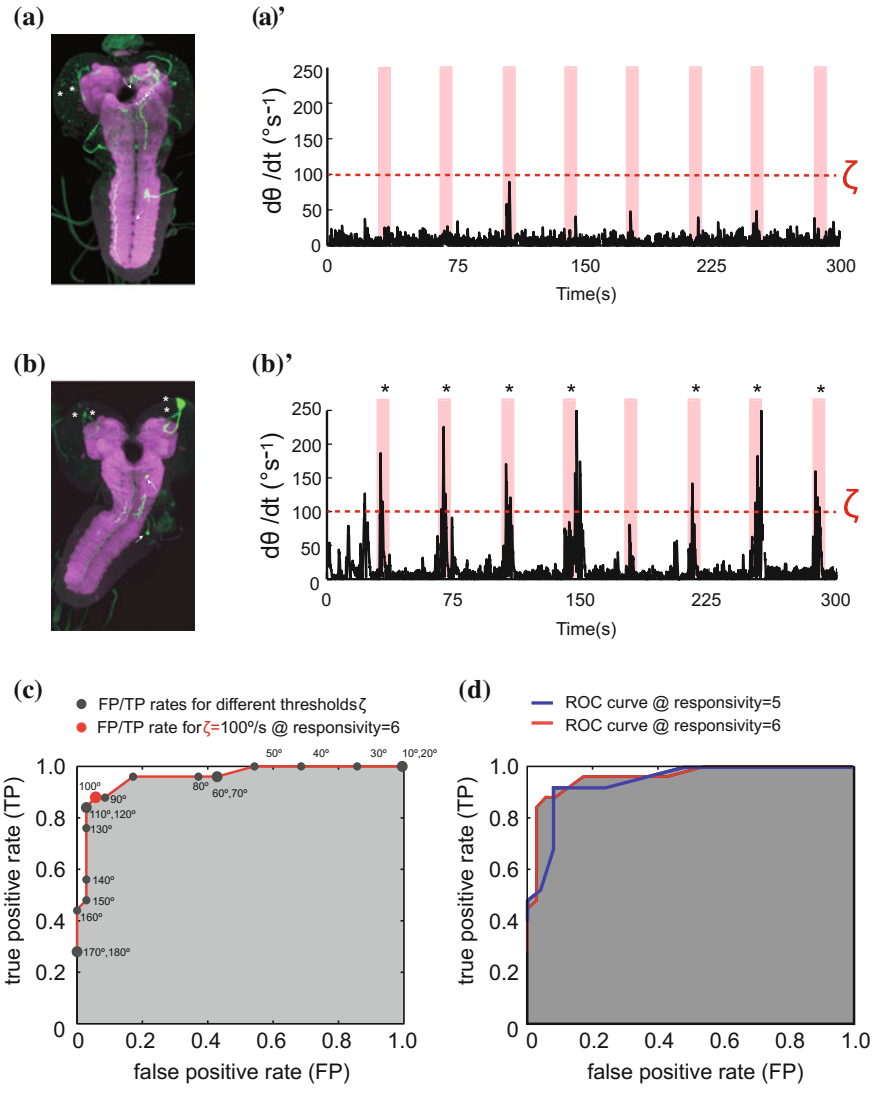

fly stock since FLP expression is restricted to differentiated neurons. Thus, one can easily combine this fly stock with any Gal4 line to perform stochastic gain-of-function experiments, which makes this approach more suited for screening purposes. For both flip-out methods, we were able to reliably visualize the morphology of the labeled neurons by performing traditional immunostaining against mVenus protein with anti-GFP antibodies (Fig. 6.5a, b).

6.5 Acute Activation of Stochastically Labeled Neurons: Stochastic Gain of Function of Neurons in the NP4820 Driver Line

Drosophila larval chemotaxis mainly involves alternation of runs (forward movements by waves of peristaltic contractions) and lateral head sweeps (head casts) followed by directed turns (Gomez-Marin et al. 2011). In a loss-of-function behavioral screen, we identified a Gal4 driver line (NP4820) with a reasonably sparse expression pattern. Activating these neurons by thermogenetics induced transient increases in head sweeps suggesting that NP4820-positive neurons are involved in run-to-turn transitions. Unfortunately, NP4820 labels multiple cell types in the brain lobes, the SEZ and the ventral nerve cord (VNC). Therefore, we applied a stochastic activation method to define which neurons covered by the NP4820 line are responsible for triggering turning maneuvers.

We opted for optogenetic activation for several reasons. First, we observed that larvae with neural activation induced by thermogenetics (dTrpA1) failed to maintain the gain-of-function behavior—an increase in head sweeps—over several seconds. Upon thermogenetic activation of NP4820 neurons, larvae engaged in fast crawling after a short bout of increase in head angular speed (Fig. 6.2c). It is possible that fast crawling results from innate avoidance triggered by high temperatures. It is equally plausible that strong activation of the neurons expressing dTrpA1 leads to a depolarization block in the neurons inducing head sweeps. Second, we were not able to reliably induce head-sweep behavior over several trials (Fig. 6.2b). To limit the identification of false positives, the reproducibility of the behavioral response over several trials is crucial. A separate technical constraint came from the fact that we could not use the blue light activated Channelrhodopsin 2 as the excitation light evoked strong head sweeps in wild type larvae (Kane et al. 2013). Therefore, we expressed CsChrimson::mVenus in NP4820 neurons. NP4820>CsChrimson::mVenus larvae robustly responded to multiple flashes of red light (Fig. 6.3d). In contrast with NP4820>CsChrimson::mVenus larvae, wild type larvae only rarely responded to a series of consecutive flashes of red light at low and moderately high intensities (3 and 18 W/m^2, Fig. 6.3a, b). We reasoned that optogenetic activation using CsChrimson would fulfill the conditions to perform stochastic gain of functions.

We took advantage of the basal leakiness of the heat shock promoter at 23 °C to induce low levels of flippase expression. With this reagent, we restricted CsChrimson expression to 1–5 neurons in individual larvae (clones, Fig. 6.5a, b). Each clone was tested with a stimulation protocol of 8 flashes of 6 s at an intensity of 18 W/m^2 and a wavelength of 625 nm (Fig. 6.3d). Individual flashes were separated by 30 s. Unlike with dTrpA1, we did not observe a decrease in the average head angular speed during consecutive gains of function (data not shown). Larval brains were dissected, fixed and immunostained for anatomical assessment with confocal imaging immediately after the behavioral experiments. To determine the behavioral phenotype of a clone, we implemented a statistical framework based

on receiver operating characteristic (ROC) to optimize a binary classifier (Duda et al. 2001) that could discriminate individual larvae that showed the gain-of-function behavior (true positive, TP clones, Fig. 6.5b') from the negative clones (true negative, TN, Fig. 6.5a'). We combined two conditions to define TP and FP (false positive), and calculate the rate of each class of events. First, we tested different threshold values (ζ) on the head angular speed—the head angular speed reveals the increase in head activity associated with turning events—and computed the TP and FP rates for each threshold value (Fig. 6.5c). Second, we evaluated how the TP and FP rates changed for different criteria on the number of flashes leading to an increase in the head angular speed that exceeded the threshold (ζ) (Fig. 6.5d).

Using this approach, we were able to draw eight ROC curves each representing different criteria on the minimum number of expected responses to the 8 light flashes (two of them are shown in Fig. 6.5d). The best performance was observed at a threshold ζ of 100°/s of the head angular speed and with a minimum response to 6 out of the 8 light flashes (responsivity = 6, Fig. 6.5c). We made use of this classifier to define the phenotype of each clone. This classifier was also used to define the expected rate of TP and TN by testing positive and negative controls (original Gal4 line driving expression of CsChrimson::mVenus and parental control devoid of Gal4 driver, respectively). Upon behavioral tests, larvae of the positive and negative controls as well as individual clones were immunostained against the mVenus protein tagging CsChrimson using a commercial antibody against GFP (product number: A-11120, Invitrogen). We tested a total of 70 gain-of-function clones out of which we identified 10 positive hits. This ratio of 10/70 was well above the expected FP rate (3–4 larvae out of 70, for calculation see Fig. 6.5c). The expression pattern of a light-responsive positive clone and a light-indifferent negative clone is illustrated in Fig. 6.5a, b. Finally, we determined the groups of neurons that were labeled more frequently than expected from the FP rate. Those neurons were assumed to be responsible for the gain-of-function phenotype. This stochastic gain-of-function strategy allowed us to narrow down the neurons responsible for the control of run-to-turn transitions to three neurons in the SEZ that were not present in any of the negative clones that had been imagined.

6.6 Closing Remarks

Neural circuits form the computational units of brains. The pace at which neural circuits are identified and functionally studied has largely accelerated in *Drosophila* after the creation of large collections of driver lines that cover sparse subsets of neurons (Pfeiffer et al. 2008; Bidaye et al. 2014). The expression patterns of a large fraction of these two collections have been reported in the adult fly (Jenett et al. 2012) as well as in the larva (Li et al. 2014). Given the relatively small number of neurons that form the larval nervous system (approximately 10,000 neurons), hopes are high that a driver line labeling each neuron can be identified. With the ability to monitor genetically labeled neurons and to reproducibly interfere with their

function, "*Drosophilists*" have now at their disposal an extraordinary toolkit to ask how neural circuits contribute to the organization of stereotyped behaviors in the larva. However, experience has shown that this toolkit is imperfect in multiple ways: most Gal4 lines label neurons belonging to more than one lineage. Expression patterns are far from being deterministic: significant variability can be observed across individuals. While these limitations should not undermine the success of massive efforts to characterize the function of neurons of the larval brain in an unbiased way (Vogelstein et al. 2014; Tastekin et al. 2015), they call for caution in the interpretation of functional manipulations.

Variability in the expression pattern of driver lines should be viewed as the rule rather than the exception. Consequently, the action of an effector might differ substantially across individual larvae. It should be common practice to characterize the expression pattern of a given driver with different reporters (Fig. 6.1). The consistency of expression patterns should be compared across different samples as well. Inter-individual variability in the expression of an effector can produce phenotypic diversity at the level of a population of larvae undergoing the same loss-of-function or gain-of-function manipulations. In the case of thermogenetics and optogenetics, the gain-of-function manipulations might also be affected by the signal that gates neural activity—a change in temperature or light intensity (Figs. 6.2a, b and 6.3a, b). The contribution of innate responses should be accounted for and, if significant, it should be subtracted from the behavior induced by the effector. In our experience, this type of analysis necessitates to be grounded in rigorous computational analysis of behavior (Egnor and Branson 2016). In light of the variability inherent to behavioral control, searching for the neural correlate of a particular phenotype must start with the definition of metrics that robustly characterize the manifestation of a certain behavior. In the absence of such quantitative metrics, a screen or more refined manipulations are unlikely to yield conclusive results. The reader should also bear in mind that behaviors tend to form a continuum that cannot always be approximated by discrete states or actions (Szigeti et al. 2015). In larvae, forward runs can be easily told apart from stops and backward runs. By contrast, the difference between head casts and turns is more arbitrary.

The typical absence of driver lines labeling a single neuron has also led the field to develop strategies to pin down the expression pattern of a line with broad coverage. The most elegant approach consists in intersecting two different driver lines with Spit-Gal4 to restrict Gal4 activity to a single neuron (Aso et al. 2014; Hampel et al. 2015; Ohyama et al. 2015). This method, however, relies on the generation of complementary lines, which is often not feasible. In their absence, we argue that the expression pattern of the original driver line can still be reduced through clonal strategies. We reviewed two variants of the flip-out method and illustrated its application to conduct clonal gain-of-function manipulations. Through this approach, we were able to map a phenotype—the sensorimotor control of turning maneuver—onto three neurons located in the SEZ whereas the original Gal4 lines labeled over 50 neurons in different regions spanning the mushroom bodies and the VNC (Tastekin et al. 2015). Interestingly the three remaining neurons included one descending neuron that projects to the VNC.

Although the flip-out method did not allow us to refine the mapping beyond this resolution, nothing guarantees that the phenotype arises from a single neuron. As stated at the beginning of this section, brains are organized by a network of neural circuits rather than isolated cells that carry each a different function. Extrapolating the function of a neural circuit through the manipulation of single cells might be limited since the function of individual neurons is often multiplex. The challenge that lies ahead of the reconstruction of neural circuits is to monitor the integrated function of specific circuits to explain the properties that emerge from their interactions.

References

Asahina K, Watanabe K, Duistermars BJ, Hoopfer E, Gonzalez CR, Eyjolfsdottir EA, Perona P, Anderson DJ (2014) Tachykinin-expressing neurons control male-specific aggressive arousal in Drosophila. Cell 156(1–2):221–235

Aso Y, Hattori D, Yu Y, Johnston RM, Iyer NA, Ngo TT, Dionne H, Abbott LF, Axel R, Tanimoto H, Rubin GM (2014) The neuronal architecture of the mushroom body provides a logic for associative learning. eLIFE 3:e04577

Baines RA, Uhler JP, Thompson A, Sweeney ST, Bate M (2001) Altered electrical properties in Drosophila neurons developing without synaptic transmission. J Neurosci 21(5):1523–1531

Bidaye SS, Machacek C, Wu Y, Dickson BJ (2014) Neuronal control of Drosophila walking direction. Science 344(6179):97–101

Clark MQ, McCumsey SJ, Lopez-Darwin S, Heckscher ES, Doe CQ (2016) Functional genetic screen to identify interneurons governing behaviorally distinct aspects of Drosophila larval motor programs. G3 (Bethesda) 6(7):2023–2031

Duda RO, Hart PE, Stork DG (2001) Pattern classification. Wiley, New York

Ebrahim SA, Dweck HK, Stokl J, Hofferberth JE, Trona F, Weniger K, Rybak J, Seki Y, Stensmyr MC, Sachse S, Hansson BS, Knaden M (2015) Drosophila avoids parasitoids by sensing their semiochemicals via a dedicated olfactory circuit. PLoS Biol 13(12):e1002318

Egnor SE, Branson K (2016) Computational analysis of behavior. Annu Rev Neurosci 39:217–236

Fenno L, Yizhar O, Deisseroth K (2011) The development and application of optogenetics. Annu Rev Neurosci 34:389–412

Gepner RM, Skanata M, Bernat NM, Kaplow M, Gershow M (2015) Computations underlying Drosophila photo-taxis, odor-taxis, and multi-sensory integration. eLIFE 4

Gerber B, Stocker RF (2007) The Drosophila larva as a model for studying chemosensation and chemosensory learning: a review. Chem Senses 32(1):65–89

Gomez-Marin A, Stephens GJ, Louis M (2011) Active sampling and decision making in Drosophila chemotaxis. Nat Commun 2:441

Gonzalez-Bellido PT, Wardill TJ, Kostyleva R, Meinertzhagen IA, Juusola M (2009) Overexpressing temperature-sensitive dynamin decelerates phototransduction and bundles microtubules in Drosophila photoreceptors. J Neurosci 29(45):14199–14210

Gordon MD, Scott K (2009) Motor control in a Drosophila taste circuit. Neuron 61(3):373–384

Green CH, Burnet B, Connolly KJ (1983) Organization and patterns of inter- and intraspecific variation in the behaviour of Drosophila larvae. Anim Behav 31(1):282–291

Hampel S, Franconville R, Simpson JH, Seeds AM (2015) A neural command circuit for grooming movement control. eLIFE 4:e08758

Hartenstein V, Younossi-Hartenstein A, Lovick JK, Kong A, Omoto JJ, Ngo KT, Viktorin G (2015) Lineage-associated tracts defining the anatomy of the Drosophila first instar larval brain. Dev Biol 406(1):14–39

Hernandez-Nunez L, Belina J, Klein M, Si G, Claus L, Carlson JR, Samuel ADT (2015) Reverse-correlation analysis of navigation dynamics in Drosophila larva using optogenetics. eLIFE 4

Hwang RY, Zhong L, Xu Y, Johnson T, Zhang F, Deisseroth K, Tracey WD (2007) Nociceptive neurons protect Drosophila larvae from parasitoid wasps. Curr Biol 17(24):2105–2116

Inagaki HK, Jung Y, Hoopfer ED, Wong AM, Mishra N, Lin JY, Tsien RY, Anderson DJ (2014) Optogenetic control of Drosophila using a red-shifted Channelrhodopsin reveals experience-dependent influences on courtship. Nat Methods 11(3):325–332

Jenett A, Rubin GM, Ngo TT, Shepherd D, Murphy C, Dionne H, Pfeiffer BD, Cavallaro A, Hall D, Jeter J, Iyer N, Fetter D, Hausenfluck JH, Peng H, Trautman ET, Svirskas RR, Myers EW, Iwinski ZR, Aso Y, DePasquale GM, Enos A, Hulamm P, Lam SC, Li HH, Laverty TR, Long F, Qu L, Murphy SD, Rokicki K, Safford T, Shaw K, Simpson JH, Sowell A, Tae S, Yu Y, Zugates CT (2012) A GAL4-driver line resource for Drosophila neurobiology. Cell Rep 2(4):991–1001

Kane EA, Gershow M, Afonso B, Larderet I, Klein M, Carter AR, de Bivort BL, Sprecher SG, Samuel AD (2013) Sensorimotor structure of Drosophila larva phototaxis. Proc Natl Acad Sci U S A 110(40):E3868–E3877

Klapoetke NC, Murata Y, Kim SS, Pulver SR, Birdsey-Benson A, Cho YK, Morimoto TK, Chuong AS, Carpenter EJ, Tian Z, Wang J, Xie Y, Yan Z, Zhang Y, Chow BY, Surek B, Melkonian M, Jayaraman V, Constantine-Paton M, Wong GK, Boyden ES (2014) Independent optical excitation of distinct neural populations. Nat Methods 11(3):338–346

Li HH, Kroll JR, Lennox SM, Ogundeyi O, Jeter J, Depasquale G, Truman JW (2014) A GAL4 driver resource for developmental and behavioral studies on the larval CNS of Drosophila. Cell Rep 8(3):897–908

Luan H, Peabody NC, Vinson CR, White BH (2006) Refined spatial manipulation of neuronal function by combinatorial restriction of transgene expression. Neuron 52(3):425–436

Luo L, Gershow M, Rosenzweig M, Kang K, Fang-Yen C, Garrity PA, Samuel AD (2010) Navigational decision making in Drosophila thermotaxis. J Neurosci 30(12):4261–4272

Marella S, Mann K, Scott K (2012) Dopaminergic modulation of sucrose acceptance behavior in Drosophila. Neuron 73(5):941–950

Matsunaga T, Fushiki A, Nose A, Kohsaka H (2013) Optogenetic perturbation of neural activity with laser illumination in semi-intact Drosophila larvae in motion. J Vis Exp 77:e50513

Nern A, Pfeiffer BD, Rubin GM (2015) Optimized tools for multicolor stochastic labeling reveal diverse stereotyped cell arrangements in the fly visual system. Proc Natl Acad Sci U S A 112(22):E2967–E2976

Ohyama T, Schneider-Mizell CM, Fetter RD, Aleman JV, Franconville R, Rivera-Alba M, Mensh BD, Branson KM, Simpson JH, Truman JW, Cardona A, Zlatic M (2015) A multilevel multimodal circuit enhances action selection in Drosophila. Nature 520(7549):633–639

Olsen SR, Wilson RI (2008) Cracking neural circuits in a tiny brain: new approaches for understanding the neural circuitry of Drosophila. Trends Neurosci 31(10):512–520

Pfeiffer BD, Jenett A, Hammonds AS, Ngo TT, Misra S, Murphy C, Scully A, Carlson JW, Wan KH, Laverty TR, Mungall C, Svirskas R, Kadonaga JT, Doe CQ, Eisen MB, Celniker SE, Rubin GM (2008) Tools for neuroanatomy and neurogenetics in Drosophila. Proc Natl Acad Sci U S A 105(28):9715–9720

Pfeiffer BD, Ngo TT, Hibbard KL, Murphy C, Jenett A, Truman JW, Rubin GM (2010) Refinement of tools for targeted gene expression in Drosophila. Genetics 186(2):735–755

Pulver SR, Pashkovski SL, Hornstein NJ, Garrity PA, Griffith LC (2009) Temporal dynamics of neuronal activation by Channelrhodopsin-2 and TRPA1 determine behavioral output in Drosophila larvae. J Neurophysiol 101(6):3075–3088

Rosenzweig M, Kang K, Garrity PA (2008) Distinct TRP channels are required for warm and cool avoidance in Drosophila melanogaster. Proc Natl Acad Sci U S A 105(38):14668–14673

Schleyer M, Reid SF, Pamir E, Saumweber T, Paisios E, Davies A, Gerber B, Louis M (2015) The impact of odor-reward memory on chemotaxis in larval Drosophila. Learn Mem 22(5):267–277

Schneider-Mizell CM, Gerhard S, Longair M, Kazimiers T, Li F, Zwart MF, Champion A, Midgley FM, Fetter RD, Saalfeld S, Cardona A (2016) Quantitative neuroanatomy for connectomics in Drosophila. eLIFE 5

Schroll C, Riemensperger T, Bucher D, Ehmer J, Voller T, Erbguth K, Gerber B, Hendel T, Nagel G, Buchner E, Fiala A (2006) Light-induced activation of distinct modulatory neurons triggers appetitive or aversive learning in Drosophila larvae. Curr Biol 16(17):1741–1747

Schulze A, Gomez-Marin A, Rajendran VG, Lott G, Musy M, Ahammad P, Deogade A, Sharpe J, Riedl J, Jarriault D, Trautman ET, Werner C, Venkadesan M, Druckmann S, Jayaraman V, Louis M (2015). Dynamical feature extraction at the sensory periphery guides chemotaxis. eLIFE 4

Simpson JH (2009) Mapping and manipulating neural circuits in the fly brain. Adv Genet 65:79–143

Sweeney ST, Broadie K, Keane J, Niemann H, O'Kane CJ (1995) Targeted expression of tetanus toxin light chain in Drosophila specifically eliminates synaptic transmission and causes behavioral defects. Neuron 14(2):341–351

Szigeti B, Deogade A, Webb B (2015) Searching for motifs in the behaviour of larval Drosophila melanogaster and *Caenorhabditis elegans* reveals continuity between behavioural states. J R Soc Interface 12(113):20150899

Tastekin I, Riedl J, Schilling-Kurz V, Gomez-Marin A, Truman JW, Louis M (2015) Role of the subesophageal zone in sensorimotor control of orientation in Drosophila larva. Curr Biol 25(11):1448–1460

Thum AS, Knapek S, Rister J, Dierichs-Schmitt E, Heisenberg M, Tanimoto H (2006) Differential potencies of effector genes in adult Drosophila. J Comp Neurol 498(2):194–203

Venken KJ, Simpson JH, Bellen HJ (2011) Genetic manipulation of genes and cells in the nervous system of the fruit fly. Neuron 72(2):202–230

Vogelstein JT, Park Y, Ohyama T, Kerr RA, Truman JW, Priebe CE, Zlatic M (2014) Discovery of brainwide neural-behavioral maps via multiscale unsupervised structure learning. Science 344(6182):386–392

von Philipsborn AC, Liu T, Yu JY, Masser C, Bidaye SS, Dickson BJ (2011) Neuronal control of Drosophila courtship song. Neuron 69(3):509–522

Wong AM, Wang JW, Axel R (2002) Spatial representation of the glomerular map in the Drosophila protocerebrum. Cell 109(2):229–241

Yoshikawa S, Long H, Thomas JB (2016) A subset of interneurons required for Drosophila larval locomotion. Mol Cell Neurosci 70:22–29

Zhang W, Ge W, Wang Z (2007) A toolbox for light control of Drosophila behaviors through Channelrhodopsin 2-mediated photo activation of targeted neurons. Eur J Neurosci 26(9):2405–2416

Zhang W, Yan Z, Jan LY, Jan YN (2013) Sound response mediated by the TRP channels NOMPC, NANCHUNG, and INACTIVE in chordotonal organs of Drosophila larvae. Proc Natl Acad Sci U S A 110(33):13612–13617

Zimmermann G, Wang LP, Vaughan AG, Manoli DS, Zhang F, Deisseroth K, Baker BS, Scott MP (2009) Manipulation of an innate escape response in Drosophila: photoexcitation of acj6 neurons induces the escape response. PLoS One 4(4):e5100

Zwart MF, Pulver SR, Truman JW, Fushiki A, Fetter RD, Cardona A, Landgraf M (2016) Selective inhibition mediates the sequential recruitment of motor pools. Neuron 91(3):615–628